An update on Gabor deconvolution

Gary F. Margrave, David C. Henley, Michael P. Lamoureux, Victor Iliescu, and Jeff P. Grossman

ABSTRACT

Gabor deconvolution has been updated and a new ProMAX module is released. The updates are: (1) a new method of spectral smoothing called hyperbolic smoothing; (2) a Gabor transform using compactly supported windows that improves run times by one to two orders of magnitude; and (3) a post-deconvolution time-variant bandpass filter whose maximum frequency tracks along a hyperbola in the time-frequency plane. We discuss the technical details of these improvements and present an overview of the new ProMAX module.

INTRODUCTION

Time-frequency analysis is a hot topic in applied mathematics with many new textbooks and monographs having appeared in recent years. Seismic data is particularly appropriate for this analysis because of its inherent nonstationarity, characterized by the progressive loss of high frequencies with increasing time. However, it is usually required to go beyond the simple analysis of nonstationarity and to actually process the data to render it more nearly stationary. Usually, this means performing some kind of an operation on the time-frequency decomposition (i.e. filtering) and then synthesizing a new signal by recombining the altered time-frequency components. Of the popular time-frequency analysis techniques, the *wavelet transform* is probably most popular; however, there is a great deal of interest in windowed Fourier transforms that have become known as *Gabor transforms* (Gabor, 1946, Feichtinger and Strohmer, 1998, Mertins, 1999). One reason that the Gabor transform remains popular in spite of the many advantages of the wavelet transform is that the latter does not diagonalize a local convolution operator while the former does.

Last year, we showed the fundamental concepts behind a new nonstationary deconvolution technique called Gabor deconvolution (Margrave and Lamoureux, 2001). As the name suggests, this method uses the Gabor transform to accomplish a time-frequency decomposition of a seismic trace. This Gabor spectrum is then processed in such a way that the effects of anelastic attenuation and the source signature are approximately removed. In its simplest form, this involves smoothing the magnitude of the Gabor spectrum to estimate the Gabor magnitude spectrum of the *propagating wavelet*. This is then combined with a *minimum phase spectrum*, computed in the usual way with the Hilbert transform, to completely specify the propagating wavelet. Then the Gabor spectrum of the seismic signal is pointwise divided by the estimated Gabor spectrum of the propagating wavelet. If the signal were noiseless, then an inverse Gabor transform would complete the process. However, we have found it necessary to precede the inverse Gabor transform with a time-variant bandpass filter to limit the whitened spectrum to the supposed signal band.

This process is motivated by a simple model of the constant-Q attenuation process that allows the forward-Q filter to be written as a pseudodifferential operator applied to the seismic reflectivity. We have shown that the Gabor transform approximately *factorizes* this pseudodifferential operator into a product of the Gabor transform of the reflectivity, times the time-frequency attenuation function, times the Fourier transform of the source signature.

In this paper we report on several new developments that improve the basic algorithm. First we describe a new method of smoothing the Gabor magnitude spectrum along hyperbolic paths (Iliescu and Margrave, 2001) that yields a more consistent estimate of the Gabor magnitude spectrum of the propagating wavelet. Then we describe an efficiency improvement to the Gabor transform in which we depart from Gaussian windows to smooth windows with compact support[1]. This brings a very large speedup to the Gabor transform with runtimes reducing by a factor between 10 and 100. We also discuss the use of both analysis and synthesis windows in this context. Also we describe a post-deconvolution bandpass filter whose magnitude spectrum follows hyperbolic contours in the time-frequency plane. Finally, we describe a new ProMAX module that incorporates these features.

HYPERBOLIC SMOOTHING OF THE GABOR MAGNITUDE SPECTRUM

Gabor factorization of a nonstationary trace model

We use a trace model that includes the source signature and the nonstationary effects of dissipation as predicted by the constant-Q model though it does not explicitly model multiples or stratigraphic filtering. The effect of constant-Q can be modelled as

$$s_Q(t) = \int\limits_{-\infty}^{\infty} \int\limits_{-\infty}^{\infty} \alpha_Q(\tau, f) r(\tau) e^{2\pi i f[t-\tau]} d\tau df, \qquad (1)$$

where $r(\tau)$ is the reflectivity sequence and the constant-Q transfer function is

$$\alpha_Q(\tau, f) = e^{-\pi f \tau / Q + iH(\pi f \tau / Q)}, \qquad (2)$$

where H denotes the Hilbert transform over f at constant τ. Equation (1) can be understood as a nonstationary convolution in the sense defined by Margrave (1998).

As defined by equation (1), s_Q models dissipation for an impulsive source. We apply a more general source signature with a stationary convolution and write our final nonstationary trace model as

---

[1]A function is said to have compact support if it is nonzero only within a finite close interval of the real line.

$$\hat{s}(f) = \hat{w}(f) \int\limits_{-\infty}^{\infty} \alpha_Q(\tau, f) r(\tau) e^{-2\pi i f \tau} d\tau, \tag{3}$$

where $\hat{w}$ and $\hat{s}$ are the Fourier transforms of the source signature and the nonstationary seismic trace respectively. Equation (3) is a replacement for the familiar stationary convolution model.

We have derived (Margrave and Lamoureux, 2001) an asymptotic result for the continuous Gabor transform of $s(t)$, whose Fourier transform is given by equation (3), as

$$V_g s(\tau, f) \approx \hat{w}(f) \alpha_Q(\tau, f) V_g r(\tau, f) \tag{4}$$

where the $\approx$ sign means that this is the leading term in an asymptotic series. In words, the continuous Gabor transform of our nonstationary trace is approximately equal to the product of the Fourier transform of the source signature, the constant Q transfer function, and the continuous Gabor transform of the reflectivity. Since, for fixed τ, the Gabor transform is just a Fourier transform, this is a *temporally local* convolutional model. It is a reasonable expectation that a similar relation holds for the discrete Gabor transform.

In closing, we mention the simplest stationary trace model, the convolutional model, has the seismic signal created from the convolution of the *wavelet* with the reflectivity. Since all seismic data is nonstationary, this convolution can only be a local approximation and the term wavelet must be taken to mean the propagating wavelet as it has evolved from the source to the time zone of interest. That is the wavelet must be roughly the product,

$$\hat{w}_{prop}(f) \approx \hat{w}(f) \alpha_Q(\tau_0, f), \tag{5}$$

where τ_0 refers to the centre of the zone of interest. Then, if we take a single Gabor window that spans the entire zone of interest, the Gabor transform is simply the Fourier transform and we write equation (4) as

$$\hat{s}(f) \approx \hat{w}_{prop}(f) \hat{r}(f). \tag{6}$$

Recalling the convolution theorem, we see that the inverse Fourier transform of equation (6) gives the elementary convolution model. So the stationary trace model is a special case of our nonstationary trace model.

Hyperbolic smoothing

In frequency-domain, stationary deconvolution it is assumed that the reflectivity spectrum is a much more rapidly varying function than the wavelet spectrum, and the ideal character of the reflectivity is said to be *white*. In practice, this has come to mean that if the Fourier magnitude spectrum of the reflectivity is smoothed, by convolving with a certain smoother, then the result will be a constant function. It is then argued that smoothing the Fourier magnitude spectrum of a seismic signal eliminates the contribution of the reflectivity and estimates the wavelet magnitude spectrum. The appropriate smoother, in both length and geometry, continues to be an empirical decision.

We follow this lead in Gabor deconvolution and assume that the reflectivity spectrum is more rapidly varying than any other component in the trace model. However, with reference to equation (4), there are now three terms in the trace model because the attenuation surface and the source signature are modelled separately. The simplest possible smoothing procedure is to convolve the Gabor magnitude spectrum of the seismic signal with a 2D boxcar, whose time and frequency dimensions must be chosen empirically. A major problem with this approach is that it has an amplitude equalization effect, much like an AGC, that tends to distort the estimated reflectivity. This is illustrated in Figure 1, where we have run a Gabor deconvolution on a synthetic signal whose underlying reflectivity contains a weak zone surrounded by two stronger zones. The reason that this happens is shown in Figure 2. The smoothed Gabor spectrum, that should be an estimate of the spectrum of the propagating wavelet, is clearly unphysical. A wavelet propagating in an attenuating medium cannot lose and then regain energy.

A better approach is suggested by the form of the constant-Q operator in equation (2). The magnitude of this operator in the time-frequency plane is constant along curves of $\tau f = \text{constant}$, which are hyperbolae. Thus we might expect that the average of the Gabor magnitude spectrum, taken along such hyperbolic paths, will estimate the attenuation surface (Iliescu and Margrave, 2001). Figure 3 shows the result of such a hyperbolic smoothing process. This is a much more physically plausible result than the previous one, although we regard this as estimating only the attenuation surface and not the source signature. To accomplish the latter, we divide the spectrum on the left of Figure 3 by the one on the right, thereby backing out the apparent attenuation and then average over all time and smooth slightly in frequency. The result is shown in Figure 4, while Figure 5 gives the resulting deconvolution. The hyperbolic smoother has suppressed the AGC effect and a better reflectivity estimate is the result. We have also experimented with least-squares fitting of the Q surface as reported in Grossman et al. (2002a).

Hyperbolic smoothing can be implemented in a variety of ways. We simply divide the entire τf range into about 100 intervals and sum the input samples into these bins. After computing the average value of each bin, we have 100 points on a curve that is a model for the hyperbolic average. Then for each input point in the grid, we interpolate a value from this curve.

A GABOR TRANSFORM WITH COMPACTLY SUPPORTED WINDOWS

Formulation of the discrete Gabor transform

We present a summary here. For more detail and greater rigour, see Grossman et al. (2002b).

Though the discrete Gabor transform can be formulated for very general time-frequency lattices (e.g. Feichtinger and Strohmer 1998), we choose a simpler approach because the more general approach can be computationally slow. Unlike the discrete Fourier transform that expands a signal into an orthonormal basis, the discrete Gabor transform expands into a more general construct called a *frame*. By choosing windows that form a *partition of unity* (POU), a simple Gabor frame, called a *tight* frame, can be

implemented (Grochenig, 2001, p118). Furthermore, most of the calculations can be done with an FFT so that numerical efficiency is fairly good. Let $w(t)$ be a set of windows satisfying the property,

$$\sum_{k \in \mathbb{Z}} w(t - k\Delta\tau) \equiv \sum_{k \in \mathbb{Z}} w_k(t) = 1, \qquad (7)$$

and let $g_k(t) = w_k(t)^p$ and $\gamma_k(t) = w_k(t)^q$ with $p + q = 1$. Then we define the forward discrete Gabor transform as

$$\widehat{s_k}(f) = F\left[s_k(\cdot)\right](f); \qquad s_k(t) \equiv s(t)g_k(t), \qquad (8).$$

where F is the (discrete) Fourier transform. We use the "hat" notation for the *Fourier* transform. Here notation shows the Gabor transform of $s(t)$ is the Fourier transform of the *Gabor slice* $s_k(t)$. (For simplicity, we use a continuous notation for signal, window, and Fourier transform and a discrete index for window position. For fully discrete formulae, the normal notation for discrete signals is easily employed.) The signal is recovered by the inverse discrete Gabor transform given by:

$$s(t) = \sum_{k \in \mathbb{Z}} \gamma_k(t) F^{-1}\left[\widehat{s_k}(\cdot)\right](t). \qquad (9)$$

Substitution of equation (8) into (9) shows that the signal is recovered exactly due to the property of equation (7) and $p + q = 1$.

In our previous work (Margrave and Lamoureux, 2001) we took $p = 1$ and $q = 0$ and chose the set $\{w_k(t)\}$ to be Gaussian windows such that

$$\sum_{k \in \mathbb{Z}} w_k(t) \approx 1, \qquad (10)$$

where

$$w_k(t) = \frac{\Delta\tau}{T\sqrt{\pi}} e^{-[t - k\Delta\tau]^2/T}, \qquad (11)$$

with T being the Gaussian (half) width. This approximate POU differs from 1 by an error term, dominated by $\exp(-[\pi T/\Delta\tau]^2)$, that can be made arbitrarily small by increasing the ratio $T/\Delta\tau$. For example, the maximum error is -150 decibels for $T/\Delta\tau = 1.5$ and is negligible for most practical purposes.

A new compactly supported window

We have adopted the use of the window shown in Figure 6, which we call a Lamoureux window. The Lamoureux window reaches unity at a single central point and is a kth order spline on either flank. The flanks are chosen such that a point that is δt from the beginning of the window has amplitude say a and the point that is δt from the

central peak has amplitude $1-a$. This property allows an easy construction of a POU. The Lamoureux window is given by

$$
wlam_k(x) = \begin{cases}
2^{k-1}x^k & . & 0 < x < 1/2 \\
1 - 2^{k-1}(1-x)^k & . & 1/2 < x < 1 \\
1 & . & 1 < x < L-1 \\
1 - 2^{k-1}(L-1-x)^k & . & L-1 < x < L-1/2 \\
2^{k-1}(L-x)^k & . & L-1/2 < x < L \\
0 & . & \text{otherwise}
\end{cases}
\tag{12}
$$

In comparison with a Gaussian window of the same width, the Lamoureux window is much more localized. (The width of the Gaussian is defined as its 1/e point.) In the context of the theory of the previous section, if we choose $p = q = 1/2$, then we will actually window with the square root of the Lamoureux window in both analysis and synthesis. For this reason, a 4th order Lamoureux is a natural choice so that the window can approach zero as a 2nd order curve. In contrast, if we used the popular raised cosine window, then its square root approaches zero linearly and has a discontinuous slope at its endpoints.

The use of compactly supported windows leads to great efficiencies in the Gabor transform. When using Gaussian windows, each windowed trace segment is as long as the original trace. So if n windows are required and the trace is of length, N, then the computation effort is proportional to $nN \log_2 N$. In contrast, if the compactly supported window is of length, M, where M is typically $0.1N$ or less, then the effort is $nM \log_2 M \approx .1nN \log_2 N$. So we expect at least an order of magnitude less effort.

When using Gaussian windows, the window width and increment are essentially independent. Equation (11) is a normalization formula that allows the formation of an approximate POU for any choice of Gaussian width and increment. In contrast, to form a simple POU with Lamoureux windows, the window spacing is determined by the width because the adjacent windows must have their peaks over the endpoints of the window in Figure 6. This is a minimally redundant POU (redundancy of 2). However, we can overcome this apparent obstruction to more redundant representations by simply shifting the minimally redundant partition by, say, 1/2 a window width and summing it to its originally. By this scheme, we can achieve any integral redundancy.

Figure 7 compares the Gabor transform using Gaussian windows to one using minimally redundant Lamoureux windows with the same nominal width. The Gaussian transform is very redundant (about 10-fold) and shows much higher resolution than the twice redundant Lamoureux window result. Nevertheless, both transforms can reconstruct the signal with high fidelity. In Figure 8, the Gaussian window transform is compared with a 6-fold redundant Lamoureux window transform. Now the Lamoureux window seems to give higher temporal resolution than the Gaussian but lower frequency

resolution. This is because the Lamoureux window is effectively shorter for the same width parameter.

POST-DECONVOLUTION NONSTATIONARY FILTER

Gabor deconvolution is a very aggressive tool that can whiten the Fourier spectrum out to the Nyquist frequency. Frequently, the result is simply too strongly whitened and, as in the stationary case, a post-deconvolution filter is desirable. The goal of such a filter is to bandlimit the whitened data to the frequencies where signal is sufficiently dominant (i.e. the signal band).

The signal band of a seismic signal from an attenuating medium is necessarily time variant. In the constant-Q model described by equation (2), the attenuation function describes a constant signal strength reduction along the hyperbolae defined by $\tau f = \text{constant}$. Under the assumption of a constant background noise level, the signal-to-noise ratio should also be constant along these trajectories. Therefore, we have implemented a nonstationary bandpass filter whose high-frequency cutoff follows a hyperbolic trajectory as shown in Figure 7. At early times the trajectory is altered to constant as the hyperbolic path becomes very wide.

GABOR DECONVOLUTION II—THE PROMAX MODULE

The improvements to Gabor deconvolution described above have been incorporated into a new ProMAX module called Gabor deconvolution II. While the overall structure of the module is similar to the Gabor deconvolution released by CREWES in 2001, significant algorithm differences and new parameters require further explanation. The single most significant change is the switch from the use of Gaussian windows to Lamoureux windows in the new program. Because of this change, many of the computational arrays are much smaller (small fraction of a trace length instead of a whole trace length, as in the Gaussian windowing scheme). This results in a dramatic reduction in computation time for the new algorithm. Depending upon the length and sample interval of the input traces and the window length specified by the user, the new deconvolution module can be from one to two orders of magnitude faster than the old. Because the output from the two modules is so similar, there are only a few circumstances where the old (Gaussian) algorithm might be preferable. Figure 10 shows a shot gather from the Blackfoot survey which has been deconvolved with the old Gabor deconvolution algorithm, while Figure 11 shows the same gather after deconvolution with the new module, using parameters that are as comparable as possible. The most visible differences are variations in gain which can most likely be attributed to the difference between effective window widths for the two algorithms.

Two new features which have been incorporated into both the new and the old algorithms since the 2001 release are the choice of 'hyperbolic smoothing' described above, and the option of applying a post-deconvolution, time-varying bandpass filter. The latter feature, in particular, is a natural one to incorporate into Gabor deconvolution, since time variation is integral with the Gabor spectrum, and the filter array can be applied by multiplication before synthesizing the output trace from its Gabor spectrum. In practice, the filter response is combined with the Gabor deconvolution operator before application of the operator to the Gabor spectrum of the trace.

Rather than describe the function of each parameter in the Gabor deconvolution II module, the help file (internal documentation) for the module is attached to this chapter as an appendix. Because of the significantly different windowing scheme in Gabor deconvolution II, with windows much shorter than traces, there is the potential for generating artifacts at window boundaries if certain parameters are inappropriately chosen with respect to the input data characteristics. The pertinent parameters in Gabor deconvolution II will be discussed in this context.

In the original Gabor deconvolution operation, the parameter associated with the half-width of the window determines the width of the window between the central unity amplitude point and the 1/e amplitude point on the Gaussian curve. Much of the energy of a windowed seismic trace is admitted through the localised central portion of the window, but the non-localised tails of the Gaussian admit significant energy as well. Because of the length and smoothness of the Gaussian curve, good estimates can be obtained of frequency components as low as the fundamental whose period is the trace length. In Gabor deconvolution II, however, the half-width parameter determines the width of the Lamoureux window between its central value of unity and the zero point at its edge. Since the Lamoureux function has no tails, all the analysed energy from a seismic trace is admitted through the localised window, and good estimates cannot be obtained for frequency components whose period is longer than the window width. Consequently, if the seismic trace contains strong frequency components whose period exceeds the desired window width, poor amplitude and phase estimates for these components will lead to discontinuities at the edges of windows during the synthesis phase of the deconvolution. Figure 12 shows the same Blackfoot shot gather as Figures 10 and 11, but with a window too narrow to handle the lowest frequency components of the ground roll in the central portion of the shot record. As can be seen in the deconvolved gather, when the amplitude of frequency components in the seismic signal becomes low (as a result of spherical divergence) with respect to the amplitude of the ground roll, discontinuities marking window edges can be seen. An obvious fix for this situation is either to apply a low-cut filter prior to deconvolution (as in Figure 13), or to lengthen the window. There are, however, other parameters which can be used to alleviate the problem.

Since the difficulty is due to inaccurate spectral estimates, one solution might be to take more spectral estimates and average them. This is effectively what happens if the 'window increment factor' is used to increase the number of windows and their overlap on the seismic trace. A factor of 2 doubles the estimates, 3 triples them, and so forth. While this tactic does smooth the window effects, the algorithm execution time is increased by a similar factor.

The 'slope exponent' parameter determines the exponent used in the Lamoureux window to form the symmetrical, smoothly varying window function. An exponent of 1 forms a triangular window, while exponents of 2 or higher give smooth bell-shaped curves. The higher the exponent, however, the steeper the slope of the curve and the more the window resembles a 'boxcar'. The steeper slope also shortens the effective transition zone between successive windows. The default for slope parameter is 4, so that the resulting windows have fairly steep slopes and relatively short transitions. Applying

windows with steep edges is known to contribute to edge effects, so one way of dealing with the window artifacts is to reduce the exponent of the window function. Figure 14 shows the result of decreasing the window exponent from 4 to 2, effectively making 'softer' windows with longer effective overlap.

The theory outlined earlier described the process of using the 'analysis window' for decomposing a seismic trace into its Gabor transform, and a 'synthesis' window to recreate a seismic trace from its (modified) Gabor components. The analysis window and its corresponding synthesis window are prepared by taking a root of the values of the chosen Lamoureux window function before applying it to the input trace or using it to synthesize the output trace. To satisfy the theory, the sum of the fractional roots for corresponding analysis and synthesis windows must be unity, so that the product of analysis and synthesis windows forms the Lamoureux window 'partition of unity'. The default choice of 'application exponent' is the square root (0.5), but virtually any choice between 0 and 1 can be made. Choosing the application exponent to be zero effectively forces the analysis window values to unity, a 'boxcar' function, while the synthesis windows then consist of 'undiminished' Lamoureux window functions (no root). An application exponent of unity, however, applies the undiminished Lamoureux window function for analysis windows, while the synthesis windows become 'boxcar' functions. It follows, then, that an exponent of 0.5 causes the application the square root of the Lamoureux function as both analysis and synthesis window functions. Because the application exponent directly affects the slope of the window functions applied both in analysis and synthesis, it has a direct influence on window edge effects, as well. To illustrate the effects of this parameter, Figure 15 shows the Blackfoot shot gather with the same deconvolution parameters as in Figure 11, except that the application exponent is 0 ('boxcar' analysis windows, full Lamoureux synthesis windows), whereas the exponent for Figure 11 is 0.5. Figure 16, on the other hand, shows the effect of an exponent of unity (Lamoureux analysis windows, 'boxcar' synthesis windows). It has been found empirically that for larger Lamoureux slope exponents (3 and larger), window edge effects can be minimised by choosing an application exponent equal to the reciprocal of the slope exponent. The reason for this is not fully understood. Figure 17 shows the Blackfoot shot gather with a slope exponent of 6 and an application exponent of 0.5. This should be compared with Figure 18, where an application exponent of 1/6 (0.167) has been used with the slope exponent of 6. This means that the analysis window values are the sixth root of the Lamoureux window function of slope 6 and the synthesis window values are the 5/6 power of the Lamoureux function. The analysis windows will have much 'softer' edges and longer transition zones than the synthesis windows. From this and similar experiments with 'slope exponent' and 'application exponent' parameters, it appears that it is more important to have soft analysis window edges than soft synthesis window edges. The window function seems to have more influence on the analysis stage of deconvolution than on the trace synthesis stage after deconvolution.

Gabor deconvolution tends to whiten seismic traces so much that post-deconvolution bandlimiting is usually required before display. While this may be done externally with a time-invariant filter, both versions of Gabor deconvolution now offer the option to apply a post-deconvolution time-varying filter. The important point to remember when selecting parameters for this internal filter application is that the bandlimits selected only

pertain to a time of one second (hard-wired). The bandwidth of all data above one second will increase beyond the specified bandlimits, up to a minimum time (specified by the user); and data below one second will have decreasing bandwidth down to a user-specified maximum time. Figure 19 is an example of unfiltered deconvolution output, while Figure 20 is the same shot with time-varying bandpass applied.

The only other parameter in Gabor deconvolution II that requires brief explanation is the 'corridor width' for the hyperbolic smoothing option. This parameter essentially defines a hyperbolic strip whose width is defined at each time-frequency point in the Gabor spectrum. The hyperbolic smoothing option, as explained above, is the mechanism by which Gabor deconvolution constructs a gain function to be applied to the Gabor spectrum. This gain, or more properly 'Q function', varies with both frequency and time and is obtained by a running average over all time-frequency space in the Gabor transform domain, where the running average array shape is a hyperbolic strip centred on a constant time-frequency curve, with width determined at every point by the input parameter 'corridor width'.

CONCLUSIONS

Gabor deconvolution is an effective nonstationary deconvolution that aggressively and robustly whitens seismic data. We presented several improvements to the previous algorithm. These are: (1) hyperbolic smoothing of the Gabor magnitude spectrum to estimate the attenuation surface; (2) compactly supported analysis and synthesis windows that provide a computational speedup of several orders of magnitude; (3) a post-deconvolution nonstationary bandpass filter whose high frequency tracks along a hyperbola in the time frequency plane; and (4) a new ProMAX module that implements these features.

FUTURE WORK

We are preparing a Gabor deconvolution module for the Seismic Unix (SU) environment.

ACKNOWLEDGEMENTS

REFERENCES

Feichtinger, H.G. and Strohmer, T., 1998, Gabor analysis and algorithms: Theory and applications: Birkhauser, ISBN 0-8176-3959-4.

Gabor, D., 1946, Theory of Communication: J. IEEE (London), **93(III)**, 429-457.

Grochenig, K., 2001, Foundations of time-frequency analysis: Brikhauser, ISBN 0-8176-4022-3.

Grossman, J.P., Margrave, G.F., Lamoureux, M.P., and Aggarwala, R., 2002a, Constant-Q wavelet estimation via a Gabor spectral model: CSEG Convention Expanded Abstracts.

Grossman, J.P., Margrave, G.F., and Lamoureux, M.P., 2002b, Constructing adaptive, nonuniform Gabor frames from partitions of unity: CREWES Research Report, Vol. **14** (this volume).

Iliescu, V. and Margrave, G.F., 2002, Reflectivity amplitude restoration in Gabor deconvolution: CSEG Convention Expanded Abstracts.

Margrave, G.F., 1998, Theory of nonstationary linear filtering in the Fourier domain with application to time-variant filtering: Geophysics, **63**, 244-259.

Margrave, G.F. and Lamoureux, M.P., 2001, Gabor deconvolution: CREWES Research Report, Vol. **13**

Mertins, A., 1999, Signal Analysis: John Wiley and Sons, ISBN 0-471-98626-7.

APPENDIX

This appendix contains the help file (internal documentation) for the Gabor deconvolution II ProMAX operation.

Gabor Deconvolution II

This module applies a technique known as Gabor Deconvolution to a panel of seismic traces, either as an ensemble, or trace-by-trace. Gabor deconvolution is a time-varying deconvolution whose operator adapts to the characteristics of the particular data captured by a time-overlapped set of windows. Gabor deconvolution II differs from its predecessor in that the windows are "Lamoureux" window functions instead of time-shifted Gaussian windows as in the original. A deconvolution operator is constructed by smoothing the magnitudes of the Gabor Transform of a seismic trace, and computing the corresponding phase. A Gabor operator array can be constructed for each trace and applied to that trace or constructed from the summed Gabor magnitudes of a trace ensemble and applied to each trace in that ensemble. Gabor deconvolution II is an experimental procedure, with several parameters which may be varied to attempt to optimize performance. This version of Gabor deconvolution has a much faster run time than the original...perhaps as much as an order of magnitude, depending upon the parameter choice.

Theory

Gabor deconvolution is based on the Gabor Transform, which is a way to analyze a seismic trace for time-varying spectral characteristics. Because this transform explicitly captures the non-stationary behavior of a seismic trace, it constitutes a natural basis for its deconvolution. The deconvolution is applied in the frequency domain by performing a complex division of the Gabor Transform by the derived deconvolution operator. The time-dependency of the resulting array is removed by summing over the time-gate dimension of the array.

Usage

Gabor deconvolution is intended for use either on individual traces or ensembles of traces. The traces can be pre-stack or post-stack traces. Data most suited to this application are those on which time-varying phenomena are superimposed (various types of noise), or which show visible non-stationarity (isolated "bright" events, loss of bandwidth with time, etc.). Because there are many parameters to select, the default values have been chosen to allow reasonable results to be obtained from Gabor deconvolution with no intervention by the user. However, the performance can usually be considerably enhanced by experimenting with the parameters.

Choose single trace or ensemble mode

This switch determines whether Gabor deconvolution is derived and applied one trace at a time, or whether the summed Gabor Transform of a whole ensemble of traces is used to derive an operator, which is then applied to each of the traces in the ensemble. The ensemble mode may not be appropriate for entire shot or receiver gathers with large offset ranges, but such gathers can be decomposed into smaller ensembles having limited offset ranges; and such ensembles may be appropriate for doing deconvolution on data which is non-stationary in both time and offset.

Restore trace amplitude levels on output

Each input data trace is automatically scaled by its average absolute amplitude to condition the data against arithmetic difficulties due to extremely large or small values. This switch parameter allows the user to choose whether or not to de-scale by the same value upon output from the algorithm. (This feature is currently disabled, 2Aug02, and is not displayed)

Half-width of the analysis/synthesis window

This is the half-width in seconds of the Lamoureux window functions used for analysis and synthesis of the data traces. Since the Lamoureux functions have a finite width between their zero amplitude points, the half-width is half the distance between the zero amplitude points, not the 1/e amplitude points as in Gaussian functions.

Window increment factor

Lamoureux windows are properly overlapped and normalized if the start point (zero amplitude) of one window coincides with the centre of the preceding window, and the end point (also zero amplitude) coincides with the centre of the succeeding window. In order to keep this proper window normalization, the increment between windows may be decreased only by applying additional properly overlapped sets of windows, offset from the original windows by increments evenly divisible into the original window width. Hence an increment factor of 2 generates an additional overlapped set of windows, offset from the original set by one fourth of the window width; an increment factor of 3 generates two additional overlapped sets of windows, the second and third offset from the first by 1/6 and 1/3 of the window width, respectively, and so forth. Proper normalization is maintained by dividing the windowed data by the window increment factor, which is equal to the total number of unity-normalized sets of overlapped windows used to sample the data. Using a value greater than one appears to stabilize the result, particularly on noisy data.

Factor to extend window before FFT

This factor is applied to the window length to determine the actual length of the FFT used to analyze the windowed trace segment. The trace segment is extended by this factor, then further extended to the next largest power of two prior to the FFT.

Pad input traces before windowing

This is a switch parameter which determines whether or not the input traces are padded before windowing, to diminish end effects. If this switch is set to true, the following parameter is used to determine the length of pad to be added to both beginning and end of the traces. The pad values are random noise whose level is set to -300 dB of the rms amplitude level of the current trace, in order that windows never encounter an all-zero trace segment.

Fraction of window width for trace padding

If the switch above is set to true, this parameter is used to determine the number of pad values to append to either end of the trace. The recommended value is more than half a window width, to move end effects off the visible seismic trace.

Slope exponent for Lamoureux window function

This integer is used as an exponent in the computation of the values of the Lamoureux window. Its default value of 4 is a relatively safe choice. Larger values can lead to window artifacts under conditions of high noise, low signal level, and small window overlap.

Application exponent for analysis window

Prior to being applied to the input trace, the values of the analysis window function are raised to this power (actually a root, since the value must be .LE. 1.0). The values of the synthesis window function are then raised to the complementary power (1.0 minus application exponent). A value of 0.5 applies a square root window to both analysis and synthesis; one applies a full strength analysis window and no synthesis window; zero applies no analysis window function and a full strength synthesis window.

Choose type of spectrum for wavelet estimate

This parameter chooses whether the Fourier Transform or the Burg algorithm is used to compute the spectral magnitudes used to construct the deconvolution operator. The Burg algorithm is somewhat slower than the FFT, if used with many coefficients.

Number of coefficients for Burg spectrum

This parameter only appears if Burg spectra are used in the decon operator. In general, the more coefficients, the more detail the Burg spectrum contains. Since the spectra are smoothed to obtain the decon operator, a small number of coefficients (3-5) will often be more effective than a larger number (10) and will run somewhat faster as well. Using a small coefficient number is similar to applying more smoothing, so the spectral smoothing parameters below can be smaller in this case.

Choose minimum or zero phase deconvolution

While a minimum phase decon would be the norm here, zero phase can be chosen, and it takes less time to construct the operator.

Choose hyperbolic time-frequency or 2-D boxcar smoothing

This parameter is used to determine the wavelet estimation method. If hyperbolic smoothing is chosen, the input Gabor spectrum is smoothed along hyperbolae of constant time-frequency to yield a Q-factor spectrum, which is then removed from the Gabor spectrum before estimating the wavelet spectrum by 2-D boxcar smoothing. If boxcar smoothing is chosen the hyperbolic smoothing step is omitted, but a constant-Q pre-whitening may be applied prior to wavelet estimation, instead.

Choose corridor width of hyperbolic smoothing in Hz-sec

This parameter determines how much smoothing occurs in the constant time-frequency method. A wide corridor applies more smoothing, forcing more of the time-dependency into the subsequent wavelet estimation. This parameter appears only if the above parameter selects for hyperbolic smoothing.

Enter estimated Q for pre-conditioning

Often, trace amplitudes are poorly conditioned...they have too large a dynamic range to be handled properly by spectral techniques without numerical instability. One way to alleviate the problem is to "pre-whiten" the data by applying a time and/or frequency dependent scale factor to reduce the dynamic range of a data array prior to spectral computations, then to remove the same scale factor after processing. In the Gabor algorithm, such a factor is applied, simulating the removal of inelastic absorption; the so-called Q-filter. The parameter here is simply the estimated Q value for the data. In this case, the estimate can be a "guesstimate", since it's just a processing parameter. Values between 20 and 200 seem to be effective. The default is set to 1.0e06 so that the effect is NO application of pre-whitening. Care has been taken to apply the pre-whitening function only to the data values, NOT to the zones of the Gabor transform which contain random noise padding. This parameter is only shown if hyperbolic smoothing (and Q-estimation) is NOT chosen above

Choose number of passes of smoothing

Smoothing is applied to the magnitude array in both the frequency and time directions. Since the smoothing operator is a uniform weight "boxcar", other types of weighting can be used by applying the boxcar more than once in succession (twice gives triangular weighting, for example). This parameter determines how many times the smoothing is applied in BOTH directions.

Choose the type of boxcar smoothing to use

The standard smoothing is simply the running mean, but the choice of the running median is also offered, for data expected to have isolated spectral peaks and notches to be smoothed. Use of median smoothing can lead to wrap-around artifacts in the output.

Wavelet smoothing window length in seconds

Determines the number of spectral magnitude points to be smoothed in time.

Choose whether to apply post-decon T-varying filter

A time-varying bandpass may be applied to the deconvolved Gabor spectra prior to collapsing them to a seismic trace. This parameter allows this filter to be applied or not. Since the post-decon filter is time-varying, its bandlimit parameters are designated at one point in time (one second), then varied to fit the constant-Q model of seismic absorption, constrained by Nyquist limits and minimum bandwidth specifications. (The high frequency parameters are not allowed to exceed 75% Nyquist for the -3 dB point or 100% Nyquist for the -80 dB point. In addition, the -3 dB high frequency point is not allowed to be less than 3.0 times the low frequency -3 dB point, and the -80 dB high frequency point cannot be less than the -3 dB high frequency point plus a third of the -3 dB bandwidth.)

Choose zero or minimum phase for filter

The post-decon time-varying filter may be chosen to be either zero or minimum phase, using this parameter.

Select low frequency -80 dB point at one second in Hz.

This parameter is the low frequency point on a Gaussian curve that is -80 dB down from the maximum spectral amplitude.

Select low frequency -3 dB point at one second in Hz.

This parameter is the low frequency point on a Gaussian curve that is -3 dB down from the maximum spectral amplitude.

Select high frequency -3 dB point at one second in Hz.

This is the -3 dB frequency for the high frequency end of the post-decon time-varying bandpass (Gaussian curve).

Select high frequency -80 dB point at one second in Hz.

This is the -80 dB frequency for the high frequency end of the post-decon time-varying bandpass (Gaussian curve).

Begin time in seconds for Q estimation or time-varying bandpass

This parameter determines the time before which estimated Q factor is constant, also the time before which time-varying bandpass parameters are held constant.

End time in seconds for Q estimation or time-varying bandpass

This parameter determines the time after which estimated Q factor is constant, also the time after which time-varying bandpass parameters are held constant.

Stability factor for spectral division operations

This parameter determines the fraction of the maximum spectral magnitude to be added to all spectral magnitudes to prevent any division by zero. The same factor is used as an additive to the Q-factor pre-whitening, and it is used in the minimum phase

computation for the post-decon time-varying bandpass filter. The default value is a safe option.

References

G. Margrave, M. Lamoureux, D. Henley

FIGURES
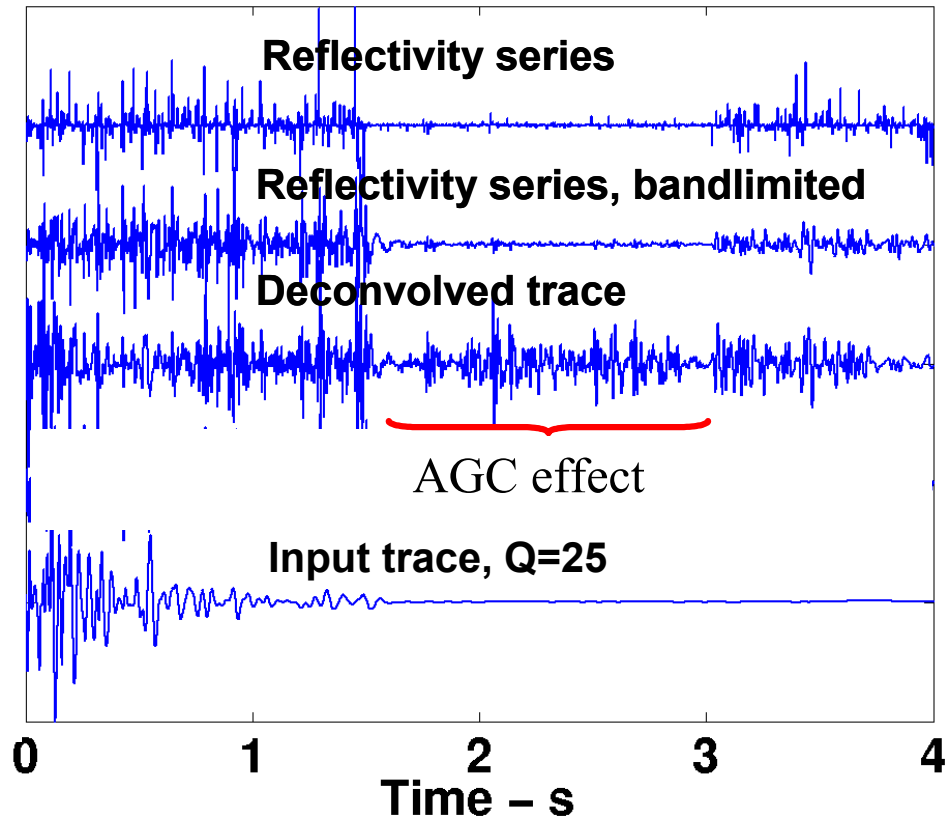
FIG. 1: A reflectivity series consisting of a quiet zone between two normal zones (top) has been modelled as a nonstationary signal and then deconvolved using boxcar smoothing. The result (second trace from bottom) as an AGC effect in that the quiet zone has been boosted to match the surrounding zones.
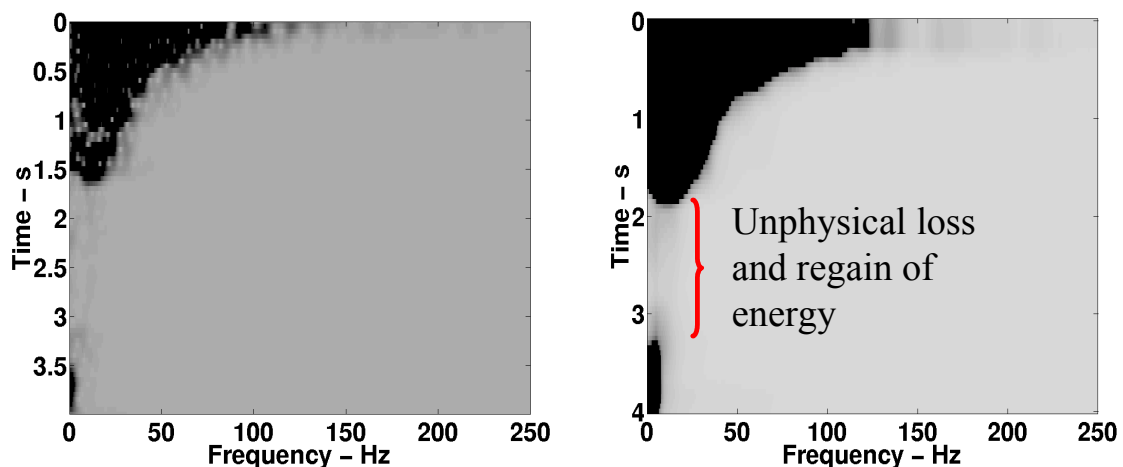

FIG. 2: On the left is the Gabor magnitude spectrum of the input trace of Figure 1. On the right is the result of smoothing the spectrum on the left with a boxcar (10 Hz by .5 sec).
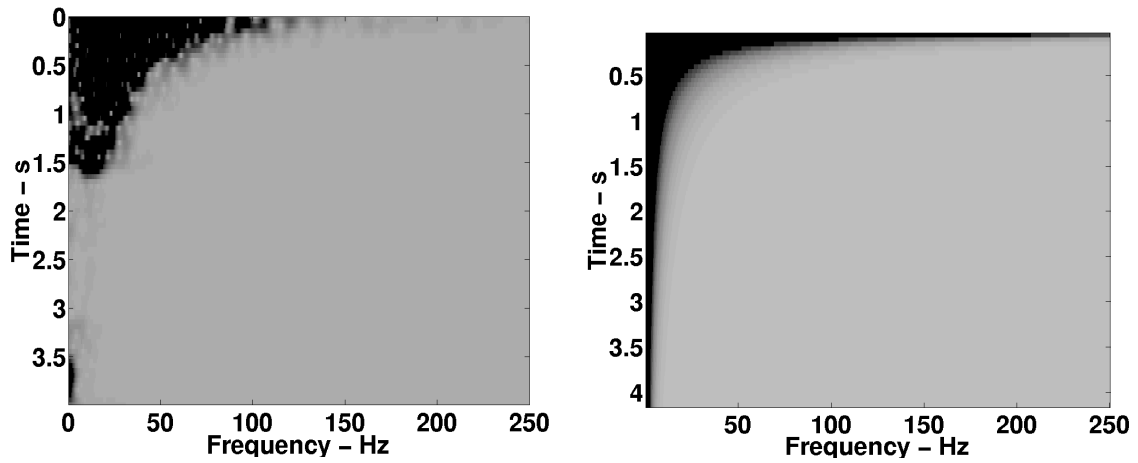
FIG. 3: On the left is the Gabor magnitude spectrum of the input trace of Figure 1. On the right is the result of smoothing the spectrum on the left along hyperbolic trajectories of the form $\tau f = \text{constant}$.
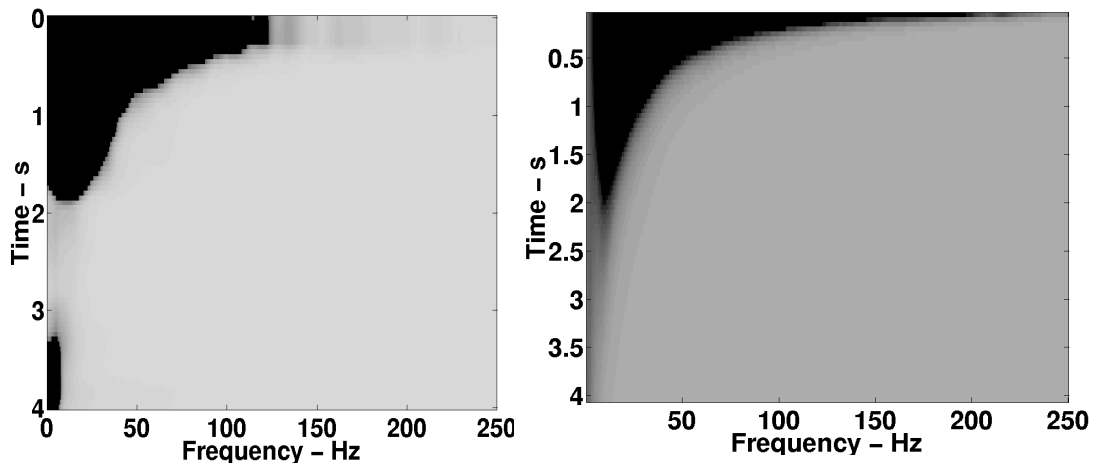
FIG. 4: The Gabor magnitude spectrum of the propagating wavelet as estimated by boxcar smoothing (left) and by hyperbolic smoothing (right).
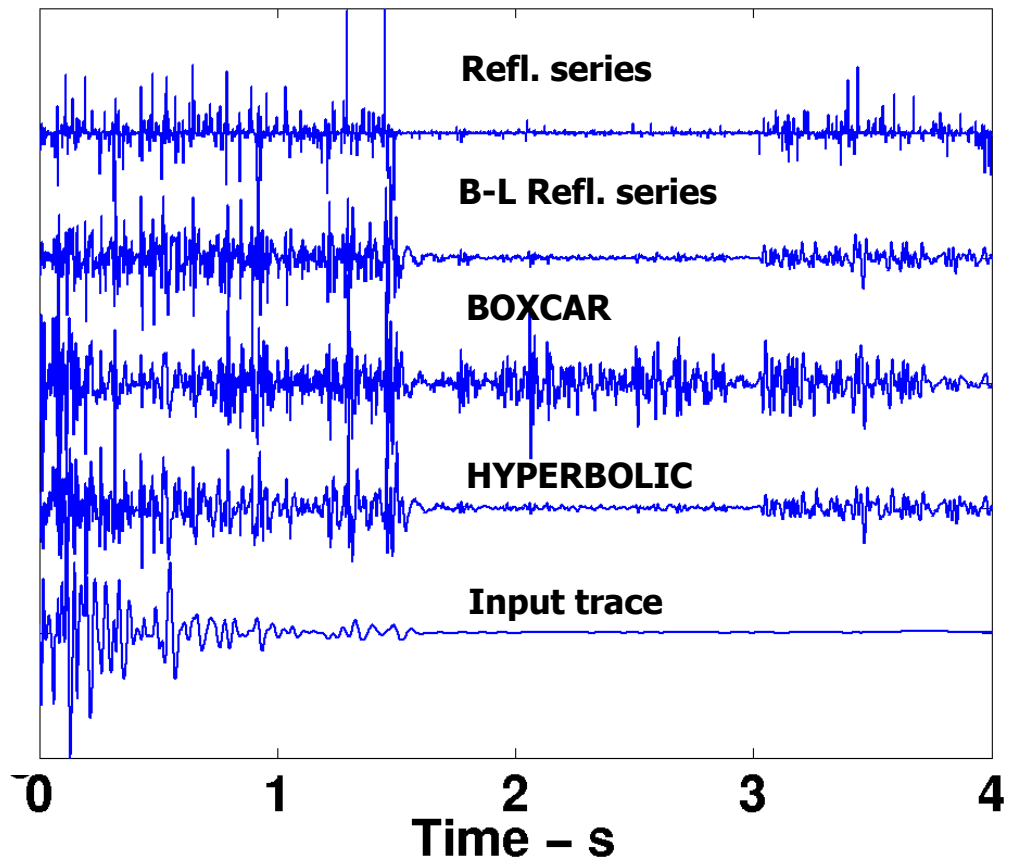
FIG. 5: Comparison of Gabor deconvolution with boxcar smoothing and with hyperbolic smoothing.
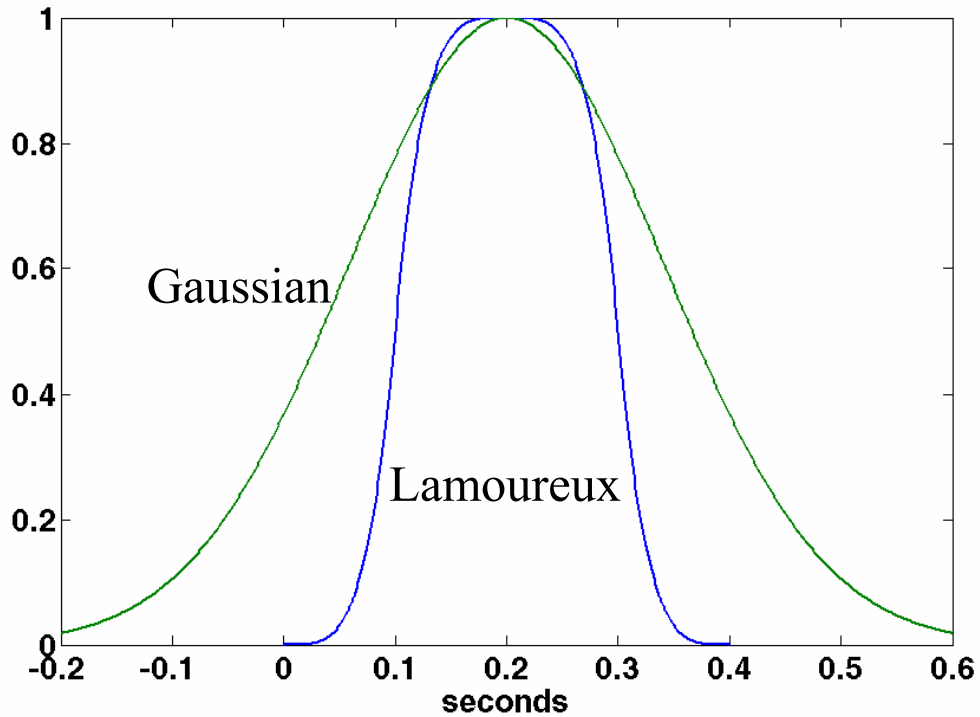
FIG. 6: Comparison of Lamoureux and Gaussian windows of the same "width". The Lamoureux window vanishes outside its width while the Gaussian only drops to 1/e at its width. The Lamoureux window is of order 4.
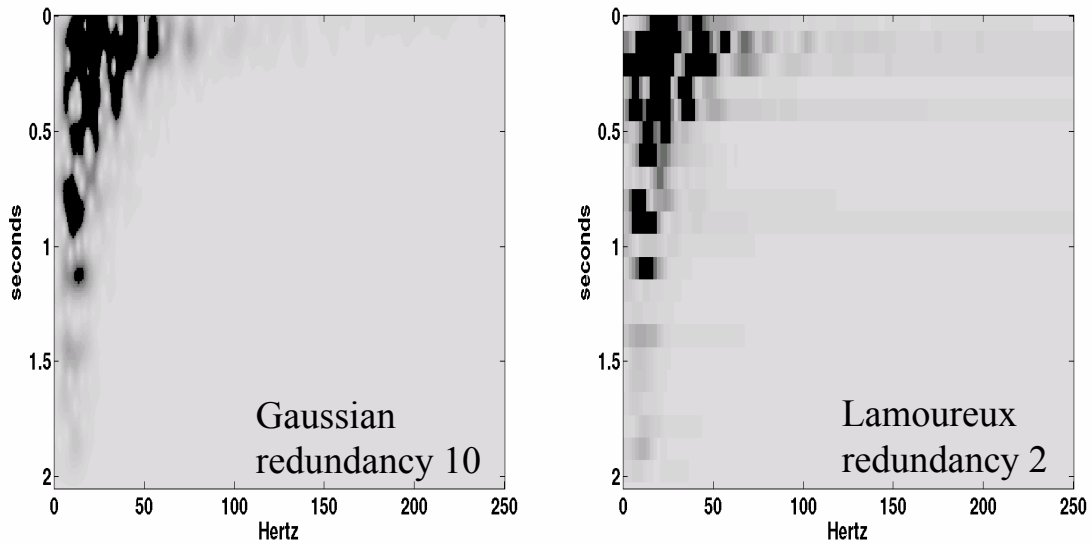
Fig. 7: Comparison of Gabor spectra with Gaussian windows (left) and Lamoureux windows (right).
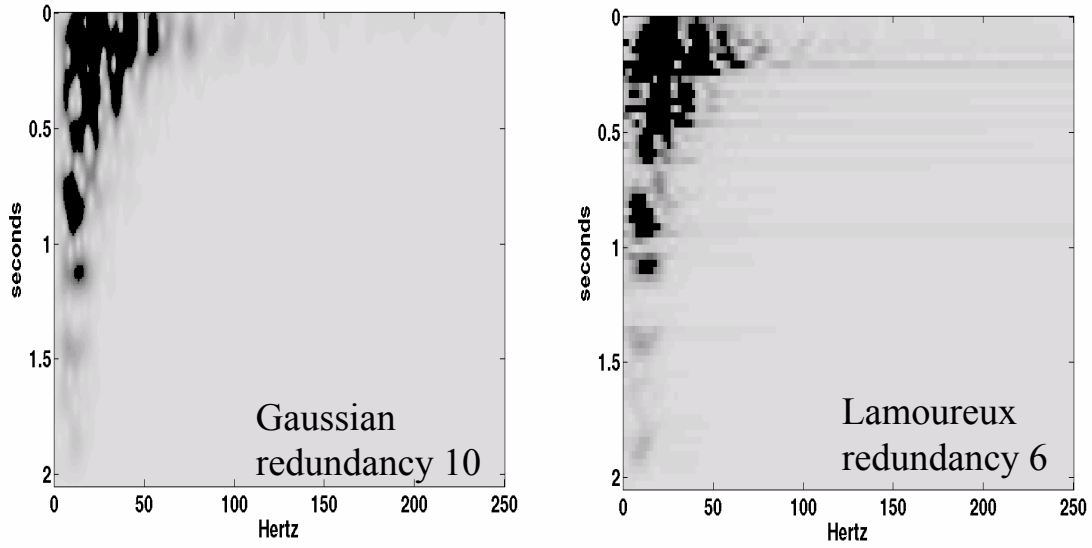
FIG. 8: Comparison of Gabor spectra with Gaussian windows (left) and Lamoureux windows (right).
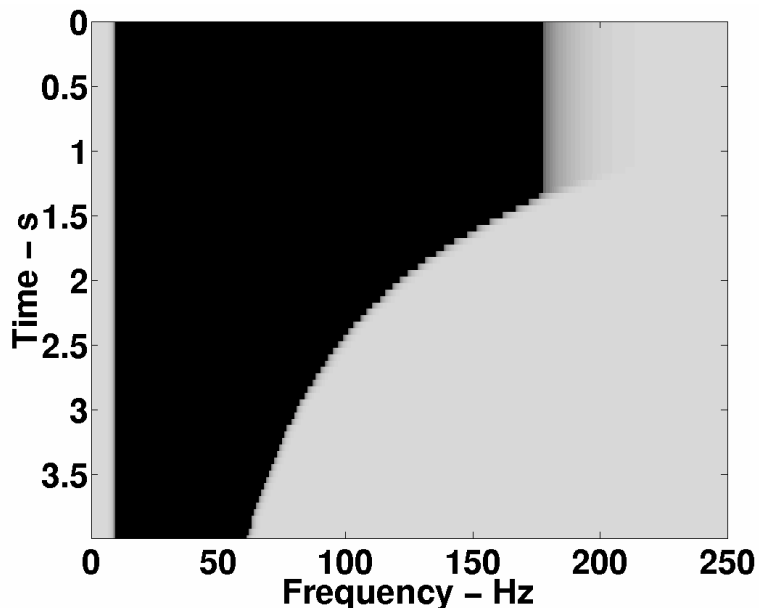
Fig. 9: The magnitude spectrum of a hyperbolic, nonstationary bandpass filter.

Gabor deconvolution—Gaussian windows
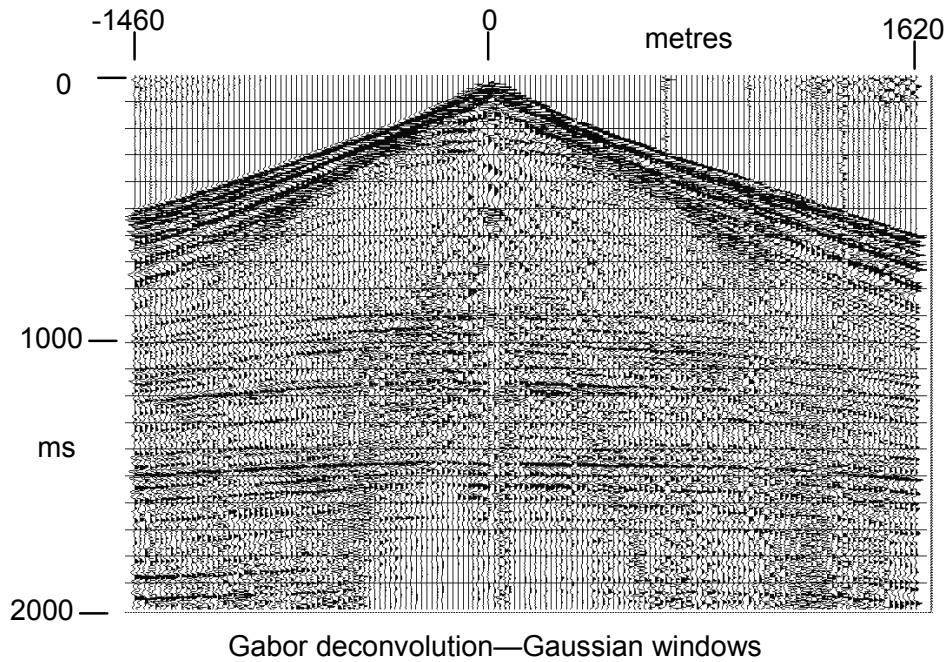
FIG. 10: Blackfoot shot gather showing application of Gabor deconvolution I, with Gaussian analysis windows, window half-width 0.2 seconds.

Gabor deconvolution—Lamoureux windows
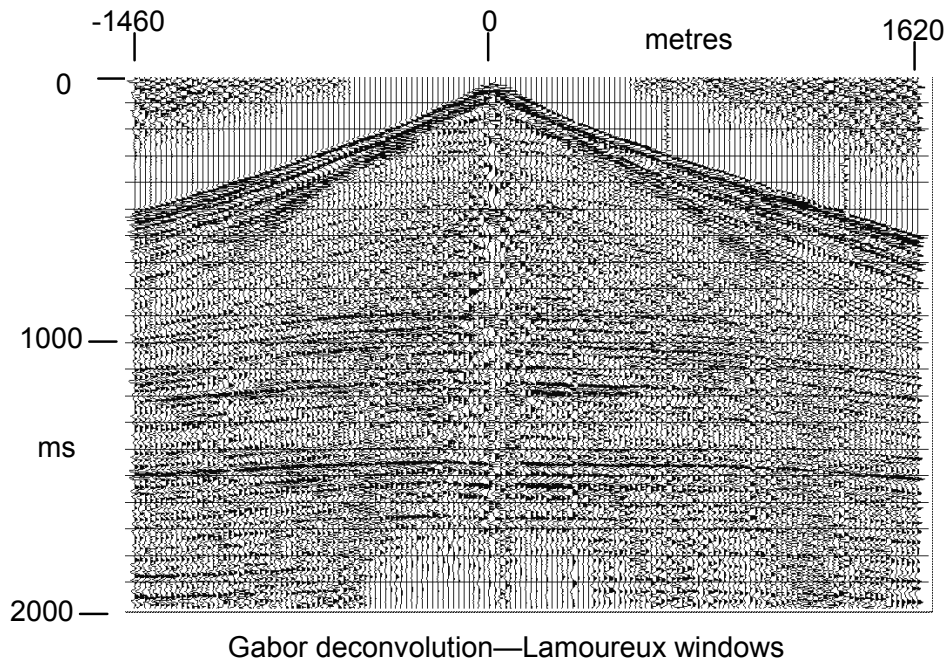
FIG. 11: Blackfoot shot gather showing application of Gabor deconvolution II, with Lamoureux analysis windows, window half-width 0.2 seconds.
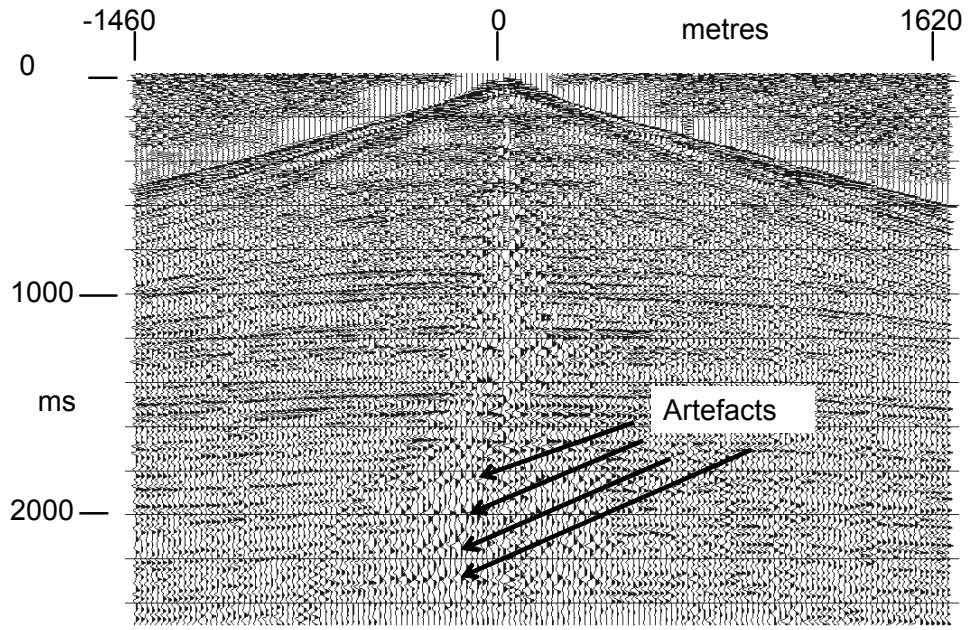
Gabor decon II—window too short—edge artefacts

FIG. 12: Artifacts caused by using an analysis window half-width too short for the low-frequency content of the noise on the shot gather.
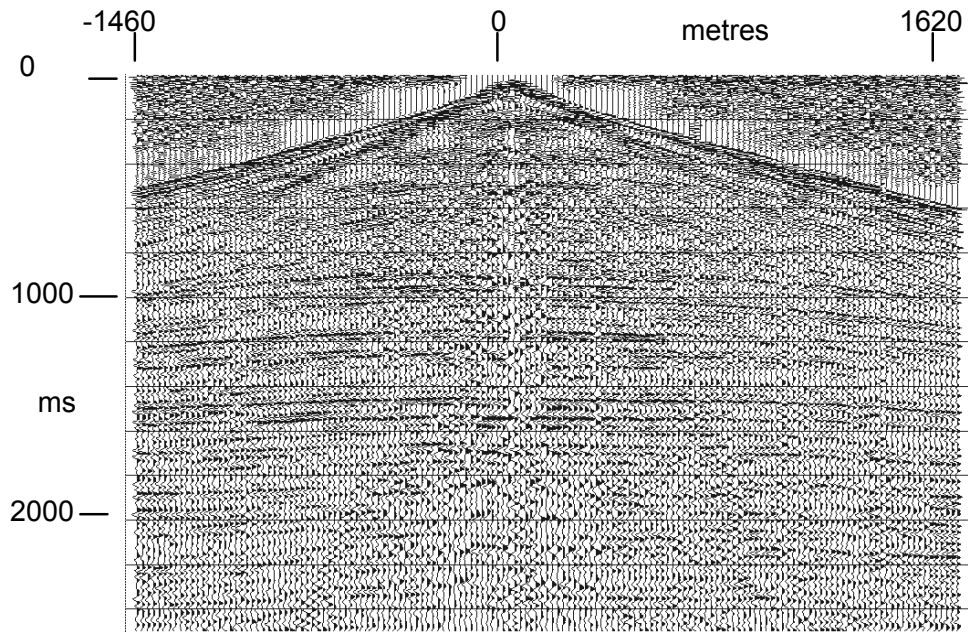
Gabor decon II—pre-filter—no edge artefacts

FIG. 13: Window artefacts removed by pre-filtering shot gather with low-cut filter.
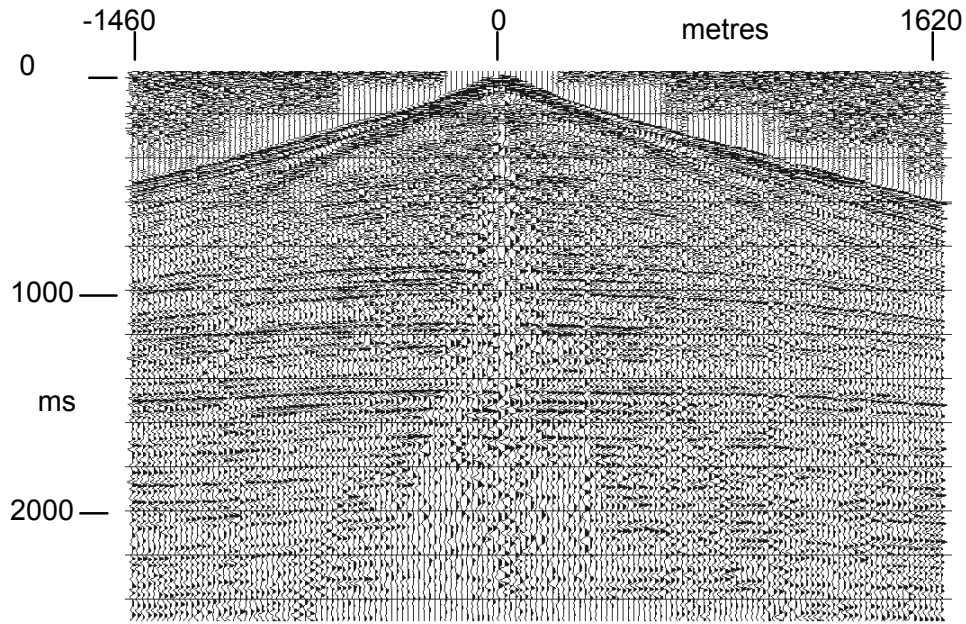
Gabor decon II—reduced window slope—no edge artefacts

FIG. 14: Window artifacts diminished by reducing slope of window edges from exponent of 4 to exponent of 2.
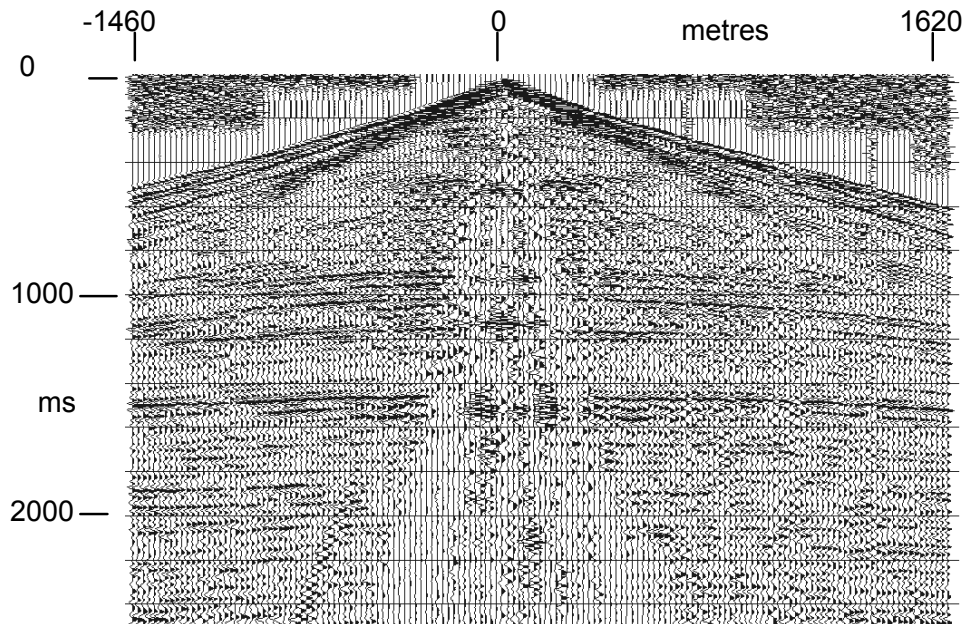
Gabor decon II—boxcar analysis window—Lamoureux
synthesis window

FIG. 15: Shot gather showing the effects of applying boxcar analysis windows and Lamoureux synthesis windows.
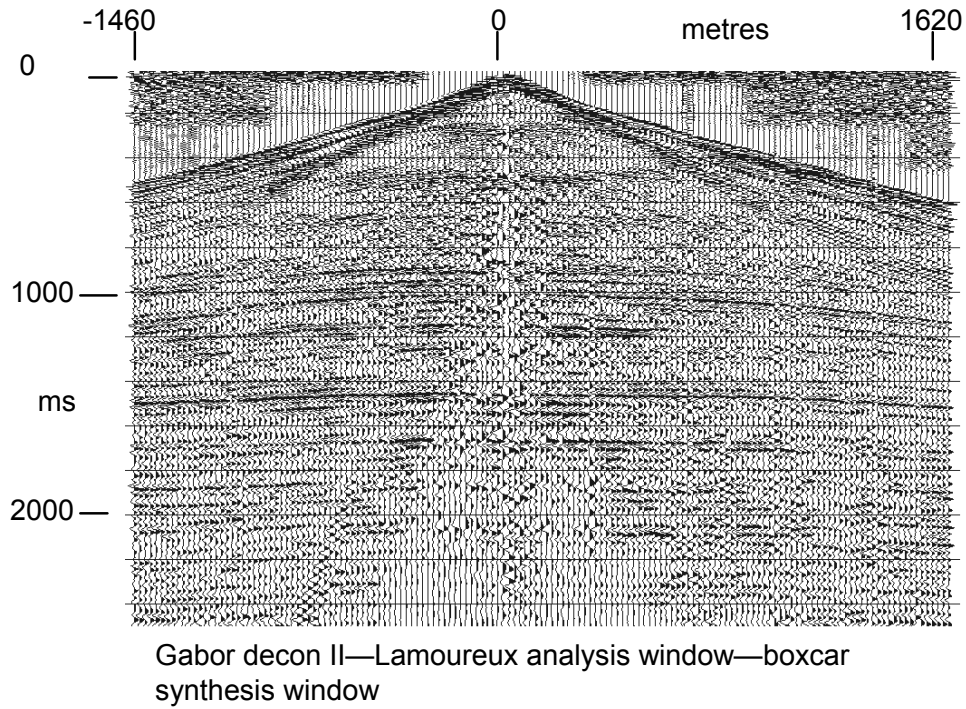
Gabor decon II—Lamoureux analysis window—boxcar synthesis window

FIG. 16: Shot gather showing the effects of applying Lamoureux analysis windows and boxcar synthesis windows.
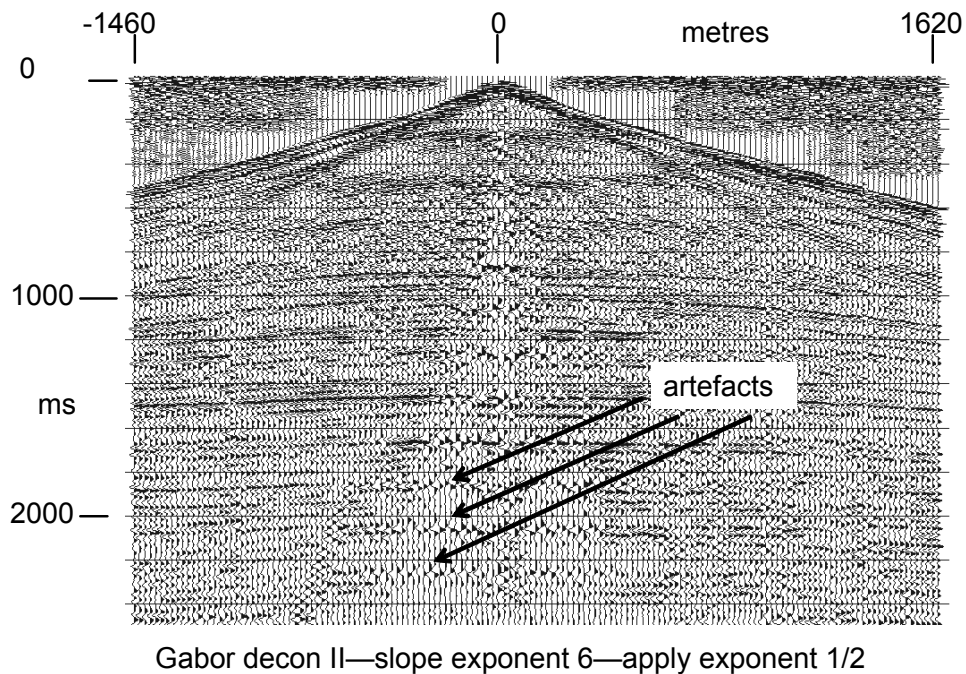

Gabor decon II—slope exponent 6—apply exponent 1/2

FIG. 17: Shot gather showing application of Lamoureux windows with slope exponent of 6 and application exponent of ½. Steep window edges lead to artifacts.
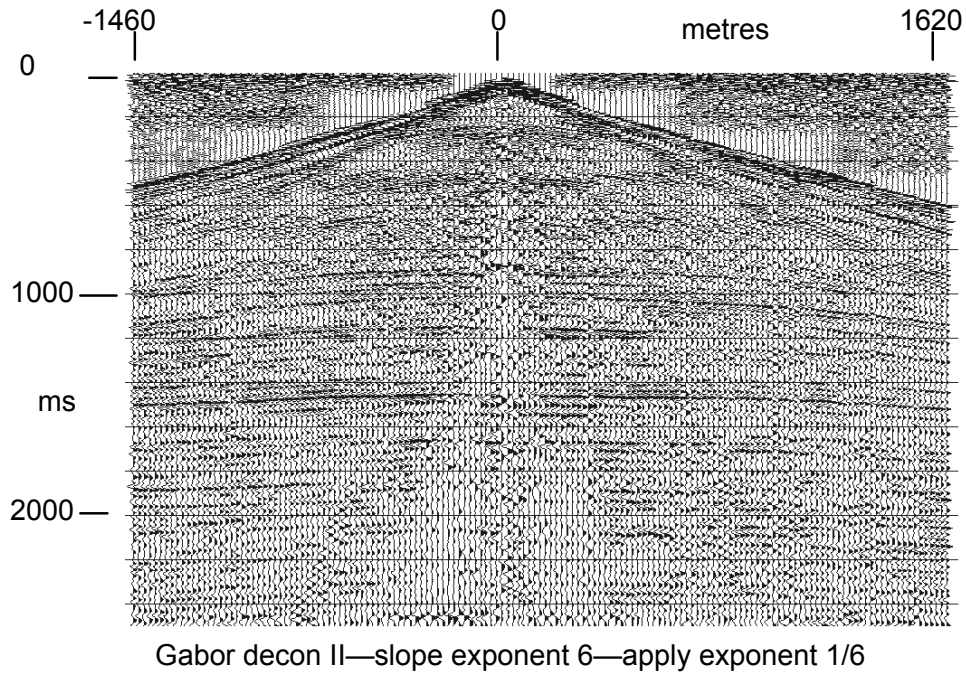
Gabor decon II—slope exponent 6—apply exponent 1/6

FIG. 18: Shot gather showing application of Lamoureux windows with slope exponent 6 and application exponent 1/6. Application exponent (root) leads to less steep window edges and reduced window artifacts.
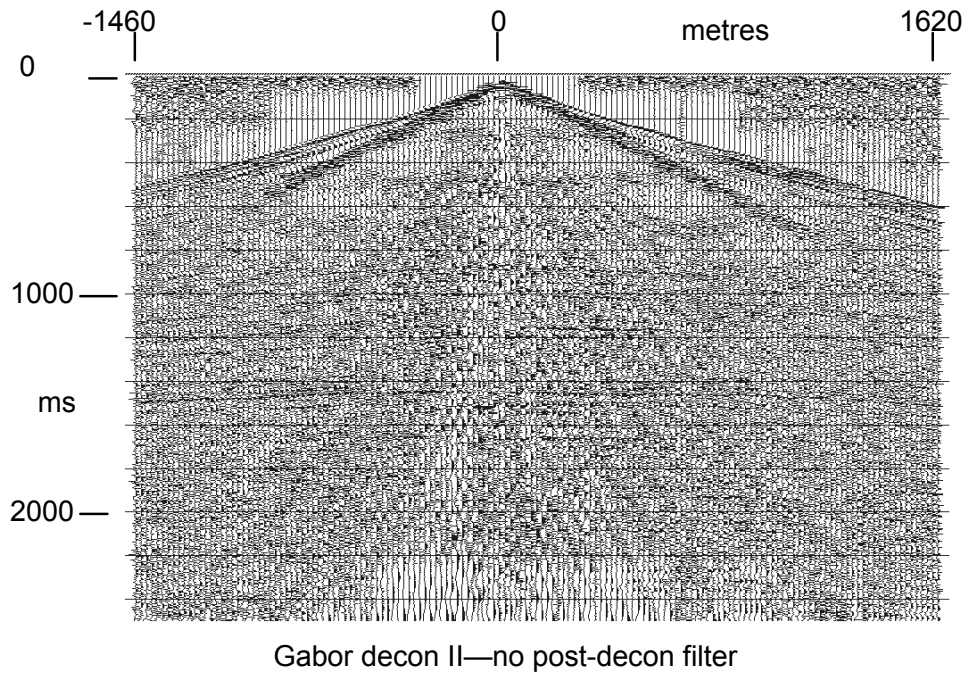

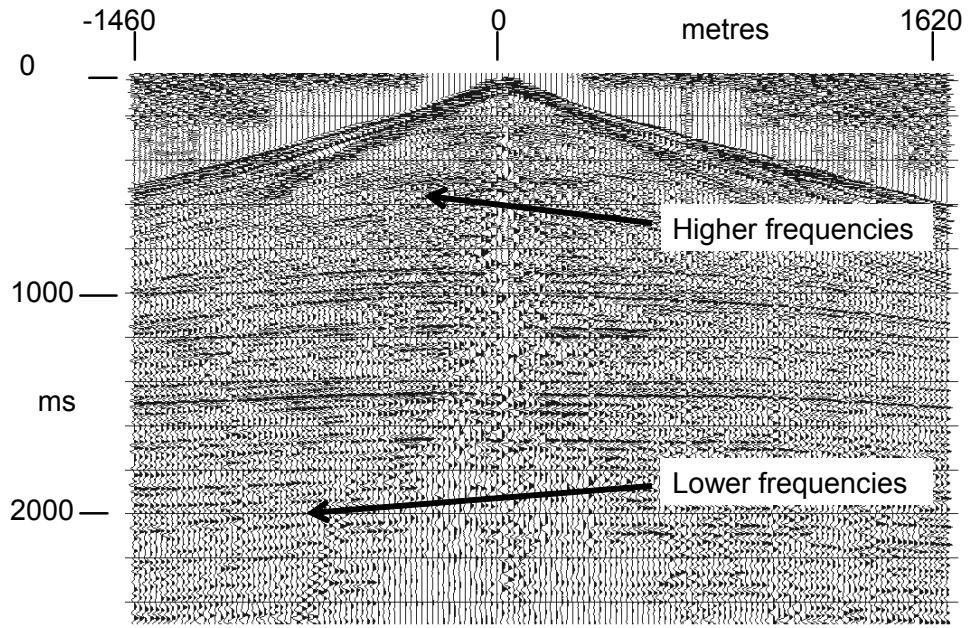Gabor decon II—no post-decon filter

FIG. 19: Gabor deconvolution II with no post-deconvolution filter. Gabor deconvolution algorithm provides abundant whitening, and output must usually be filtered.

Gabor decon II—post-decon time-varying bandpass filter

FIG. 20: Gabor deconvolution II with time-varying post-deconvolution bandpass filter applied. The time-varying frequency content of the result is quite evident.